

Biothiol Xenon MRI Sensor Based on Thiol-Addition Reaction

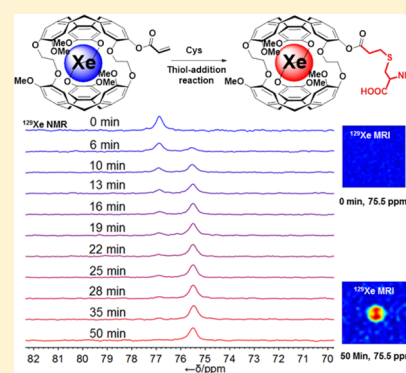
Shengjun Yang,[†] Weiping Jiang,[†] Lili Ren,[†] Yaping Yuan,[†] Bin Zhang,[†] Qing Luo,[†] Qianni Guo,[†] Louis-S. Bouchard,[‡] Maili Liu,[†] and Xin Zhou^{*,†}

[†]Key Laboratory of Magnetic Resonance in Biological Systems, State Key Laboratory of Magnetic Resonance and Atomic and Molecular Physics, National Center for Magnetic Resonance in Wuhan, Wuhan Institute of Physics and Mathematics, Chinese Academy of Sciences, Wuhan, 430071, China

[‡]Department of Chemistry and Biochemistry, California NanoSystems Institute, The Molecular Biology Institute, University of California, Los Angeles, California 90095, United States

S Supporting Information

ABSTRACT: Biothiols such as cysteine (Cys), homocysteine (Hcy), and glutathione (GSH) play an important role in regulating the vital functions of living organisms. Knowledge of their biodistribution in real-time could help diagnose a variety of conditions. However, existing methods of biothiol detection are invasive and require assays. Herein we report a molecular biosensor for biothiol detection using the nuclear spin resonance of ^{129}Xe . The ^{129}Xe biosensor consists of a cryptophane cage encapsulating a xenon atom and an acrylate group. The latter serves as a reactive site to covalently bond biothiols through a thiol-addition reaction. The biosensor enables discrimination of Cys from Hcy and GSH through the chemical shift and average reaction rate. This biosensor can be detected at a concentration of $10\ \mu\text{M}$ in a single scan and it has been applied to detect biothiols in bovine serum solution. Our results indicate that this biosensor is a promising tool for the real-time imaging of biothiol distributions.



The development of methods for the detection of biothiols such as cysteine (Cys), homocysteine (Hcy), and glutathione (GSH) is of great interest due to their crucial roles in biological processes.^{1,2} For example, abnormal Cys and Hcy levels are associated with health problems such as AIDS, Alzheimer's disease, Parkinson's, and cardiovascular diseases.^{3,4} Glutathione is an essential antioxidant that maintains redox homeostasis through the equilibrium established between free thiols and oxidized disulfides within biological systems.^{5,6}

During the past decades, considerable efforts have been devoted to developing various methods for thiol detection in vitro, including high performance liquid chromatography,^{7,8} capillary electrophoresis,^{9,10} voltammetry,^{11,12} and flow injection,^{13,14} as well as mass spectrometry.^{15,16} Unfortunately, these highly sensitive benchtop analytical tools are invasive methods and do not provide biodistributions. In recent years, several fluorescence sensors have been designed for thiol detection. These fluorescence sensors are generally based on the specific reactions,^{17–27} such as Michael addition reaction, cyclization reaction, cleavage reaction of sulfonamide, sulfonate esters, selenium–nitrogen bonds, and disulfide bonds by thiol, nucleophilic substitution reaction, and others. Although the fluorescence method shows high sensitivity, its main drawback is poor penetration depth due to light scattering in optically opaque media. This disadvantage makes fluorescence methods less suitable for imaging tissue.²⁸ Magnetic resonance imaging (MRI), on the other hand, can generate tomographic images of tissue without penetration depth limitations. However, conventional MRI images are mainly based on water proton signal and

lack chemical specificity for analytical purposes. Chemical specificity in MRI can be introduced by way of molecular sensors. Such sensors have been developed that employ modulation of relaxation rates or chemical shifts.^{29–33} However, such sensors have inherently low sensitivity. Therefore, new methods for biothiol detection and imaging would be beneficial.

A method to overcome low sensitivity problems is hyperpolarization. ^{129}Xe nuclei can be hyperpolarized by spin-exchange optical pumping to increase signal by 4–5 orders of magnitude.^{34,35} In addition, the wide chemical shift window of more than 200 ppm renders it highly susceptible to the local chemical environment, making it possible to detect biomolecules or biochemical reactions.³⁶ Several ^{129}Xe biosensors have been developed featuring a host molecular system^{37–44} encapsulating Xe atom and a targeting group for site-specific molecular recognition. Such host molecular systems based on cryptophane have been widely studied and developed for pH and temperature measurements,^{45–47} for the detection of proteins,^{48–54} enzymes,^{43,55–57} nucleic acids,⁵⁸ metal ions,^{59–61} Glycans,⁶² and transmembrane receptors.^{63–66} More recently, the concept of smart Xe biosensor has been demonstrated using a host–guest model system,⁶⁷ but not in the context of monitoring biothiol levels.

Received: January 29, 2016

Accepted: April 29, 2016

Published: April 29, 2016

Herein we report a novel biosensor to detect biothiol distributions via MRI. Detection proceeds through a thiol-addition reaction, which can be monitored by hyperpolarized ^{129}Xe NMR spectroscopy. The biosensor incorporates two parts: cryptophane cage conjugated to a ligand possessing a reactive group. Cryptophane acts as a host for the capture of xenon atoms and alters the ^{129}Xe NMR chemical shift based on binding to the ligand. The acrylate group, which is known to be involved in thiol-addition reactions to generate thioether,⁶⁸ was selected to react with biothiols. In this manner, the reaction-induced structural transformation of the biosensor alters the electron density of the cryptophane cage, resulting in a change to the chemical shift.

EXPERIMENTAL SECTION

Materials and Instruments. All chemicals and solvents were purchased from the commercial supplier and used without further purification. Column chromatography was performed using silica gel (200–300 mesh) using eluents in the indicated v:v ratio. Room temperature ^1H and ^{13}C NMR spectra were recorded in CDCl_3 , using a Bruker AMX-500 NMR spectrometer. Chemical shift (δ) are given in ppm relative to CDCl_3 (77 ppm for ^{13}C) or internal TMS (0 ppm for ^1H). High-resolution mass spectrometry (HR MS-ESI) spectra were obtained on a Bruker microTOF-Q instrument. All pH measurements were carried out using Mettler Toledo SevenEasy pH meter. The UV–visible absorption spectra measurements were performed using an Evolution 220 spectrophotometer (ThermoFisher Scientific). The melting point was measured using a SGW X-4 Melting Point Tester. All solutions and buffers were prepared with distilled water passed through Milli-Q ultrapurification system. Unless otherwise stated, the experiments were performed in HEPES buffer (4-(2-hydroxyethyl)-1-piperazineethanesulfonic acid, 20 mM, pH 7.4) solution with DMSO as cosolvent at 25 °C.

Synthesis and Characterization of Cryptophane 1. To the solution of cryptophane 2^{37,63} (29 mg, used in racemic form) and triethylamine (100 μL) in dry CH_2Cl_2 , acryloyl chloride (176 mg) in dry CH_2Cl_2 was dropped slowly under an ice–water bath. After the reaction mixture was stirred for 12 h at room temperature, the solution was washed with water (5 mL \times 3) and then dried in anhydrous Na_2SO_4 . The crude product was purified by silica gel column ($\text{CH}_2\text{Cl}_2/\text{CH}_3\text{OH} = 100:1$ (v/v)) to afford cryptophane 1. Melting point > 300 °C. ^1H NMR (500 MHz, CDCl_3): δ 6.92 (s, 1H), 6.87 (s, 1H), 6.82 (s, 1H), 6.78 (s, 1H), 6.76 (d, 2H), 6.71 (s, 2H), 6.69–6.66 (q, 4H), 6.63 (d, 0.5H), 6.59 (d, 0.5H), 6.28–6.23 (m, 1H), 6.07–6.04 (dd, 1H), 4.66–4.57 (m, 6H), 4.29–4.05 (m, 12H), 3.83–3.78 (m, 15H), 3.49–3.40 (m, 6H). ^{13}C NMR (125 MHz, CDCl_3): δ 163.79, 149.72, 149.70, 149.63, 149.61, 149.58, 148.83, 146.82, 146.81, 146.66, 146.52, 146.47, 139.87, 138.28, 134.48, 134.44, 134.18, 134.11, 133.83, 133.25, 132.83, 131.93, 131.63, 131.61, 131.26, 131.15, 127.19, 124.18, 121.40, 121.22, 121.12, 120.87, 120.51, 120.29, 114.07, 113.65, 113.61, 69.62, 69.48, 69.37, 69.31, 69.29, 69.11, 55.72, 55.64, 55.62, 55.60, 55.58, 36.53, 36.25, 36.15, 35.82. HR MS-ESI: (m/z) calcd for $\text{C}_{56}\text{H}_{54}\text{O}_{13}\text{Na}^+$ [$M + \text{Na}^+$], 957.3462; found, 957.3483.

Sample Preparation. Cryptophane 1 was dissolved into DMSO (HPLC grade) to prepare the stock solution with a concentration of 1.5 mM. Thiol stock solutions were freshly prepared prior to each experiment. Other analytes were dissolved into distilled water with a certain concentration as

stock solutions. After dilution to the desired concentration of cryptophane 1 in HEPES buffer (20 mM, pH 7.4) solution, various other analytes were added. The resulting solution was well-mixed and incubated for a certain minute at 25 °C and then prepared for the measurement of UV–visible absorption or NMR spectrometer. For NMR/MRI experiments, the resulting solution was transferred to NMR tube and placed in the magnet's bore.

^{129}Xe NMR and MRI Experiments. Hyperpolarized ^{129}Xe fluid was polarized by the spin-exchange optical pumping method with a home-built polarizer and a 86%-enriched ^{129}Xe gas mixture consisting of 2% Xe, 10% N_2 , and 88% He.^{34,61} The average value of the ^{129}Xe nuclear-spin polarization generated by this setup was about 20%. The temperature in the pumping cell was 418 K and the pressure was 47 PSI. Unless otherwise stated, the hyperpolarized gas mixture was bubbled for 60 s in a 10 mm tailor-made NMR tube containing the solution of interest at the rate of 0.08 standard liters per minute followed by a 3 s delay (to allow bubbles to collapse) prior to signal acquisition. The dissolved Xe gas did not escape significantly from the solution during the NMR measurements, as determined by measurements of the partial pressure of the Xe gas, which remained stable.

All NMR and MRI experiments were conducted on a 9.4 T NMR spectrometer (Bruker Avance 400, Ettlingen, Germany) equipped with microimaging gradient coils. The tube containing the test sample was placed in the magnet's bore and held at a temperature of 298 K by using a flow of heated N_2 gas. ^{129}Xe spectra were obtained with a 10 mm double resonant probe (^{129}Xe and ^1H , PA BBO 400 W1/S2 BB-H-D-10Z). The spectra were acquired with a rectangle pulse of flip angle (90°). Images were acquired with matrix size 64 \times 64 point images (field of view: 8 cm \times 8 cm) using a gradient echo sequence with a Gaussian pulse 20 ms long and slice thickness of 17 mm, echo time of 12.92 ms, repetition time of 26.94 ms and a 10 mm Bruker probehead (MIC WB40 RES 400 $^1\text{H}/^{129}\text{Xe}$).

For ^{129}Xe NMR experiments in bovine serum solution, each sample was added L-81 (0.1% final concentration) to reduce foaming caused by gas bubbling before ^{129}Xe NMR experiment.⁶⁴

The signals are referenced with respect to Xe gas extrapolated to zero pressure. Unless stated otherwise, the spectra were processed with the line broadening of 10 Hz.

RESULTS AND DISCUSSION

Synthesis of Cryptophane 1. As shown in Scheme 1, cryptophane 1 was obtained by the reaction of cryptophane 2 with acryloyl chloride at room temperature and characterized by ^1H NMR, ^{13}C NMR, and high-resolution mass spectroscopy (HR MS; see the Supporting Information, Figures S1 and S2).

Biosensor 1 in Response to Biothiols. The hyperpolarized ^{129}Xe NMR resonance of biosensor 1 (including cryptophane 1 and encapsulated ^{129}Xe) was studied under the conditions of 20 mM HEPES buffer (pH 7.4) with 45% DMSO (v/v) as cosolvent at 25 °C. The ^{129}Xe NMR spectrum of biosensor 1 (200 μM) shows two resonances that are assigned with dissolved free Xe at $\delta = 229.6$ ppm and caged Xe in cryptophane 1 at $\delta = 76.9$ ppm, respectively (Figure 1). The encapsulated ^{129}Xe reversibly exchanges with free ^{129}Xe with an exchange rate of about 25 Hz.^{48,49}

Upon addition of 3 equiv Cys, notably, a new signal at $\delta = 75.5$ ppm (Xe@2) appears within minutes (Figure 2). This new resonance is attributed to cryptophane 1 undergoing a thiol-

Scheme 1. Synthesis of the Cryptophane 1 and the Proposed Reaction Mechanism of Cryptophane 1 with Cys

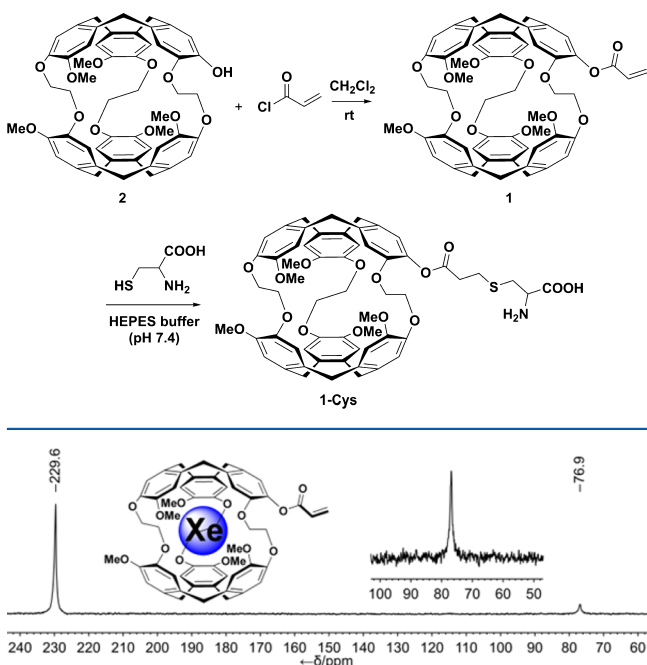


Figure 1. Single-scan ^{129}Xe NMR spectrum of biosensor 1 ($200\ \mu\text{M}$) in the test solution.

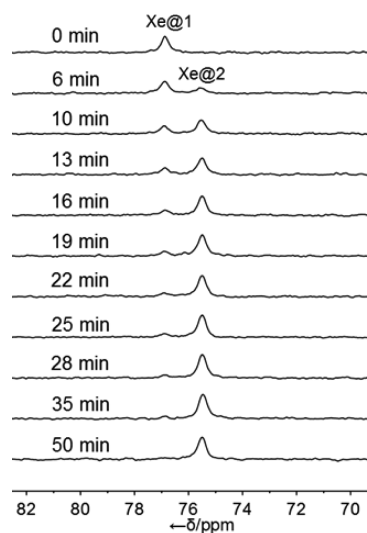


Figure 2. ^{129}Xe chemical shift change of biosensor 1 ($200\ \mu\text{M}$) upon addition of 3 equiv Cys. All spectra were obtained in the same sample at different times with a single scan.

addition reaction with Cys to produce a new cryptophane derivative. By recording ^{129}Xe NMR spectra as a function of time, the intensity of the signal at $\delta = 76.9$ ppm (Xe@1) gradually decreases in about 30 min (see the Supporting Information, Figure S3). Concomitantly, the integral intensity of the new signal at $\delta = 75.5$ ppm increases until it reaches a saturation. Obviously, the chemical shift of caged Xe gives rise to a 1.4 ppm upfield shift after the addition of Cys. A similar result was observed when treated with 1 equiv Cys (see the Supporting Information, Figure S4). Furthermore, this reaction also can proceed under the conditions of 20 mM HEPES buffer (pH 7.4) with 10% DMSO at $25\ ^\circ\text{C}$ (see the Supporting

Information, Figure S5). These results illustrate that biosensor 1 can be monitored by ^{129}Xe NMR spectroscopy. However, the absorption spectra of cryptophane 1 show no obvious change when treated with Cys (see the Supporting Information, Figure S6).

We also investigated the ^{129}Xe NMR spectra of biosensor 1 in the presence of Hcy and GSH under the same conditions. After addition of Hcy and GSH respectively, a similar ^{129}Xe NMR spectral response was observed (see the Supporting Information, Figures S7 and S8). This suggests that the reaction of cryptophane 1 with Hcy or GSH also experience a similar reaction as Cys. The new emerging signal appears at $\delta = 75.7$ ppm and is associated with an increase of 1.2 ppm (upfield) in the chemical shift. By contrast, the integral intensity of the signal at $\delta = 76.9$ ppm for Hcy and GSH takes more than 3 h to disappear (see the Supporting Information, Figure S3). That means the thiol-addition reaction rates of cryptophane 1 with Hcy ($\text{p}K_a: 8.87$) and GSH ($\text{p}K_a: 9.20$) are much slower than that of Cys ($\text{p}K_a: 8.30$), which may be ascribed to their different $\text{p}K_a$ values.⁶⁹

The above results demonstrate that biosensor 1 not only can monitor biothiols levels through ^{129}Xe NMR, but also can discriminate Cys over Hcy and GSH through chemical shift and average reaction rate (Figure 3). We also demonstrate that this

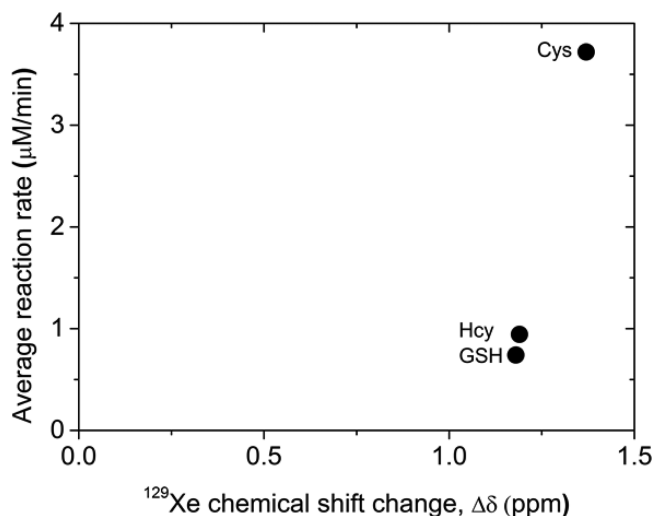


Figure 3. Average reaction rate against the ^{129}Xe chemical shift change ($\Delta\delta$) of biosensor 1 induced by Cys, Hcy and GSH, respectively. The average reaction rate value, which is determined by the change in concentration from initial to equilibrium state over that time period.

reaction-based ^{129}Xe biosensor can be imaged by MRI, thereby paving the way for a novel methodology enabling accurate spatial localization of the biothiols.

Proposed Reaction Mechanism. The chemical shift change of caged Xe is likely to be a consequence of chemical structure transformation caused by thiol-addition reaction (Scheme 1). To shed light on the mechanism, we performed time-of-flight mass spectrometry (TOF-MS) and ^1H NMR experiments (see the Supporting Information, Figures S9 and S10). The TOF-MS spectrum of cryptophane 1 with 3 equiv Cys under test conditions displays a peak at $m/z = 1056.5$, which is consistent with the molecular weight of the expected $[1-\text{Cys} + \text{H}^+]$ adduct (calcd 1056.4). Further analysis of the ^1H NMR spectrum revealed the disappearance of the resonance signals between 6.0 and 6.3 ppm upon addition of Cys to

cryptophane **1**. These resonances are assigned to carbon–carbon double bond protons. These results indicate that the acrylate group of cryptophane **1** react with the thiol of Cys to generate thioether. However, it is not identical with the reported fluorescent probe of acryloyl group with Cys (see the Supporting Information, Figure S11), which subsequently undergoes intramolecular cyclization after the thiol-addition conjugation.^{70,71}

Selectivity and Sensitivity of Biosensor 1. To evaluate the selectivity of biosensor **1** for biothiols, we carried out the experiments using a series of amino acids and various other analytes. In each case, solutions of these species were separately added to cryptophane **1** under uniform conditions and ¹²⁹Xe NMR spectra were recorded after incubating for 75 min (except for Hcy and GSH, which were incubated for 140 and 180 min, respectively). As shown in Figure 4, the ¹²⁹Xe chemical shift of

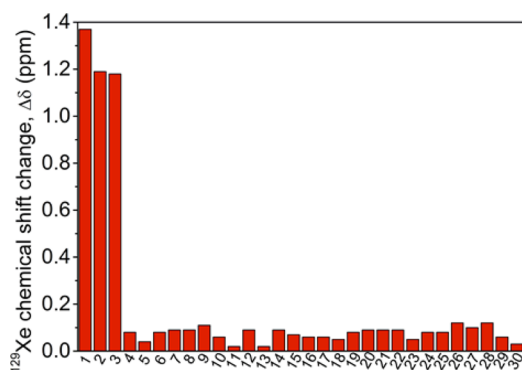


Figure 4. Chemical shift change of biosensor **1** (200 μ M) after addition of various species (1, Cys; 2, Hcy; 3, GSH; 4, phenylglycine; 5, Asp; 6, Lys; 7, Trp; 8, Gly; 9, Leu; 10, Thr; 11, Ser; 12, Met; 13, Tyr; 14, HSCH₂CH₂OH; 15, 4-methoxy thiophenol; 16, HS⁻; 17, SO₃²⁻; 18, F⁻; 19, SO₄²⁻; 20, P₂O₇⁴⁻; 21, CO₃²⁻; 22, H₂PO₄⁻; 23, Cl⁻; 24, S₂O₃²⁻; 25, OH⁻; 26, SiO₃²⁻; 27, HSO₃⁻; 28, NO₂⁻; 29, Ac⁻; 30, HCO₃⁻). Bars represent the ¹²⁹Xe chemical shift change value ($\Delta\delta$) of biosensor **1** in the absence and in the presence of each species.

biosensor **1** was significantly altered in the presence of biological thiols, whereas no obvious changes were observed upon addition of other amino acids and analytes (see the Supporting Information, Figure S12). These results illustrate that biosensor **1** has high selectivity toward biothiols and also can discriminate Cys from Hcy and GSH.

The sensitivity of this ¹²⁹Xe biosensor was also evaluated (see the Supporting Information, Figure S13). Under the test conditions, this biosensor can be detected at a concentration of 10 μ M with a single scan. Signal averaging can be used to detect lower concentrations. For example, 4096 averages enable detection of the cryptophane **1** at 80 nM levels after treatment with Cys. These results show that the sensitivity of this ¹²⁹Xe biosensor could be potentially sufficient for monitoring intracellular biothiol levels.^{72,73} Furthermore, if the HyperCEST technique could be employed, it is likely that the sensitivity may be further enhanced.⁴⁸ However, there is a challenge to using biosensor **1** with the HyperCEST technique due to the small chemical shift change.

MR Image of Cys. Owing to the chemical shift change between the signals of caged Xe in the absence and in the presence of Cys up to 1.6 ppm, we also investigated the property of biosensor **1** for ¹²⁹Xe MRI. As depicted in Figure 5A,B, a frequency-selective gradient echo sequence centered at

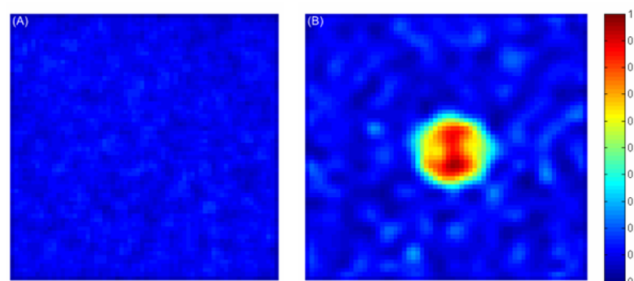


Figure 5. ¹²⁹Xe axial gradient-echo MRI images of a 10 mm tube containing (A) only 200 μ M cryptophane **1** and (B) 200 μ M cryptophane **1** treated with 3 equiv Cys for 50 min under test conditions. Images were acquired with a soft radiofrequency pulse excitation centered at $\delta = 75.5$ ppm.

75.5 ppm was used to obtain images of the biosensor **1** (A) without and (B) with Cys. The difference between images A and B illustrates that Cys can be detected and localized by ¹²⁹Xe MRI.

Biothiols Detection in Bovine Serum Solution. Finally, we checked the practicality of biosensor **1** for biothiols detection in bovine serum solution. It is clear that biosensor **1** still interacts with Cys and the ¹²⁹Xe NMR chemical shift of encapsulated Xe in the absence and in the presence of Cys exhibits distinct different signals (Figure 6). Similar results were

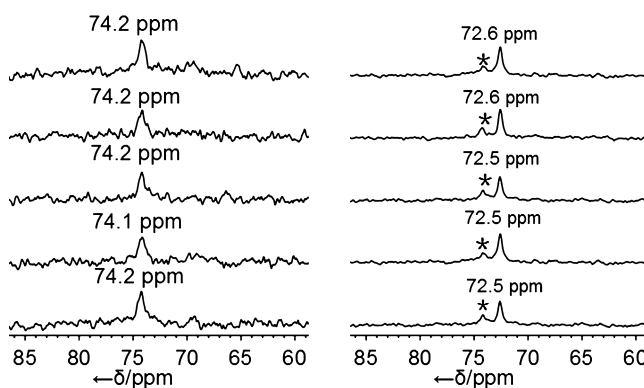


Figure 6. ¹²⁹Xe NMR spectra of biosensor **1** (40 μ M) in the absence (left) and in the presence (right) of Cys in 20 mM HEPES buffer (pH 7.4) solution (containing 10% bovine serum and 20% DMSO, v/v). The ¹²⁹Xe NMR spectra were measured independently five times. Figures in the spectra are the chemical shift of caged xenon. The ¹²⁹Xe NMR chemical shift of free xenon dissolved in the test solution is 209.7 ppm (not shown). It clearly shows the ¹²⁹Xe NMR chemical shift change of caged xenon of cryptophane **1** in the absence and in the presence of Cys is up to 1.6 ppm. The stars denote the signal of the rest biosensor **1**. Line width of the spectra is 20 Hz.

also observed when cryptophane **1** treated with Hcy and GSH (see the Supporting Information, Figure S14). Moreover, the interassay precision of biosensor **1** shows high reproducibility.

CONCLUSIONS

To the best of our knowledge, we have presented the first example of using ¹²⁹Xe NMR to monitor thiol-addition reaction. Our thiol-addition reaction-based ¹²⁹Xe biosensor for the detection of biothiols consists of a simple functionalized cryptophane host cage that can report chemical information about the binding to biothiols through the modulation of the Xe chemical shift. An acrylate group acts as a reaction site for

the covalent binding to biothiols. The selectivity for biothiols among amino acids and analytes is good, and the biosensor can also discriminate Cys from Hcy and GSH. In addition, this biosensor can be used to detect biothiols in bovine serum solution, demonstrating its potential for the detection of biothiol distributions.

■ ASSOCIATED CONTENT

■ Supporting Information

The Supporting Information is available free of charge on the ACS Publications website at DOI: [10.1021/acs.analchem.6b00403](https://doi.org/10.1021/acs.analchem.6b00403).

Characterization, absorption spectra treated with Cys, time-dependent ^{129}Xe NMR signal interacting with biothiols, ^{129}Xe spectra in response to Hcy and GSH, ^1H NMR and MS spectra and ^{129}Xe NMR spectra for reaction mechanism studies, ^{129}Xe spectra in the presence of various analytes, ^{129}Xe spectra for sensitivity, ^{129}Xe spectra in response to GSH and Hcy in bovine serum solution, and other materials are presented (PDF).

■ AUTHOR INFORMATION

Corresponding Author

*E-mail: xinzhou@wipm.ac.cn. Tel.: +86 27 87198802.

Notes

The authors declare no competing financial interest.

■ ACKNOWLEDGMENTS

This work is supported by National Natural Science Foundation of China Grants 81227902, 21302217, and 21475147. We thank Dr. Leif Schröder for helpful comments on the manuscript.

■ REFERENCES

- (1) Chen, X.; Zhou, Y.; Peng, X. J.; Yoon, J. *Chem. Soc. Rev.* **2010**, *39*, 2120–2135.
- (2) Townsend, D. M.; Tew, K. D.; Tapiero, H. *Biomed. Pharmacother.* **2003**, *57*, 145–155.
- (3) Shahrokhian, S. *Anal. Chem.* **2001**, *73*, 5972–5978.
- (4) Seshadri, S.; Beiser, A.; Selhub, J.; Jacques, P. F.; Rosenberg, I. H.; D'Agostino, R. B.; Wilson, P. W. F.; Wolf, P. A. *N. Engl. J. Med.* **2002**, *346*, 476–483.
- (5) Dalton, T. P.; Shertzer, H. G.; Puga, A. *Annu. Rev. Pharmacol. Toxicol.* **1999**, *39*, 67–101.
- (6) Wood, Z. A.; Schröder, E.; Harris, J. R.; Poole, L. B. *Trends Biochem. Sci.* **2003**, *28*, 32–40.
- (7) Vacek, J.; Klejdus, B.; Petrolova, J.; Lojkova, L.; Kuban, V. *Analyst* **2006**, *131*, 1167–1174.
- (8) Chen, W.; Zhao, Y.; Seefeldt, T.; Guan, X. J. *J. Pharm. Biomed. Anal.* **2008**, *48*, 1375–1380.
- (9) Ling, Y. Y.; Yin, X. F.; Fang, Z. L. *Electrophoresis* **2005**, *26*, 4759–4766.
- (10) Inoue, T.; Kirchhoff, J. R. *Anal. Chem.* **2002**, *74*, 1349–1354.
- (11) Calvo-Marzal, P.; Chumbimuni-Torres, K. Y.; Hoeher, N. F.; Kubota, L. T. *Clin. Chim. Acta* **2006**, *371*, 152–158.
- (12) Nezamzadeh-Ejhih, A.; Hashemi, H. S. *Talanta* **2012**, *88*, 201–208.
- (13) Waseem, A.; Yaqoob, M.; Nabi, A. *Luminescence* **2008**, *23*, 144–149.
- (14) Pérez-Ruiz, T.; Martínez-Lozano, C.; Tomás, V.; Carpena, J. *Analyst* **1992**, *117*, 1025–1028.
- (15) Burford, N.; Eelman, M. D.; Mahony, D. E.; Morash, M. *Chem. Commun.* **2003**, *7*, 146–147.

- (16) Atsriku, C.; Benz, C. C.; Scott, G. K.; Gibson, B. W.; Baldwin, M. A. *Anal. Chem.* **2007**, *79*, 3083–3090.
- (17) Yin, C. X.; Huo, F. J.; Zhang, J. J.; Martínez-Mañez, R.; Yang, Y. T.; Lv, H. G.; Li, S. D. *Chem. Soc. Rev.* **2013**, *42*, 6032–6059.
- (18) Wang, J.; Liu, H. B.; Tong, Z. F.; Ha, C.-S. *Coord. Chem. Rev.* **2015**, *303*, 139–184.
- (19) Jun, M. E.; Roy, B.; Ahn, K. H. *Chem. Commun.* **2011**, *47*, 7583–7601.
- (20) McMahon, B. K.; Gunnlaugsson, T. *J. Am. Chem. Soc.* **2012**, *134*, 10725–10728.
- (21) Han, C. M.; Yang, H. R.; Chen, M.; Su, Q. Q.; Feng, W.; Li, F. Y. *ACS Appl. Mater. Interfaces* **2015**, *7*, 27968–27975.
- (22) Niu, W. F.; Guo, L.; Li, Y. H.; Shuang, S. M.; Dong, C.; Wong, M. S. *Anal. Chem.* **2016**, *88*, 1908–1914.
- (23) Miao, Q. Q.; Li, Q.; Yuan, Q. P.; Li, L. L.; Hai, Z. J.; Liu, S.; Liang, G. L. *Anal. Chem.* **2015**, *87*, 3460–3466.
- (24) Zhang, J. J.; Wang, J. X.; Liu, J. T.; Ning, L. L.; Zhu, X. Y.; Yu, B. F.; Liu, X. Y.; Yao, X. J.; Zhang, H. X. *Anal. Chem.* **2015**, *87*, 4856–4863.
- (25) Lv, H.; Yang, X. F.; Zhong, Y.; Guo, Y.; Li, Z.; Li, H. *Anal. Chem.* **2014**, *86*, 1800–1807.
- (26) Lim, S.-Y.; Hong, K.-H.; Kim, D. I.; Kwon, H.; Kim, H.-J. *J. Am. Chem. Soc.* **2014**, *136*, 7018–7025.
- (27) Bao, Y.; Li, Q.; Liu, B.; Du, F.; Tian, J.; Wang, H.; Wang, Y.; Bai, R. *Chem. Commun.* **2012**, *48*, 118–120.
- (28) Rice, B. W.; Cable, M. D.; Nelson, M. B. *J. Biomed. Opt.* **2001**, *6*, 432–440.
- (29) De Leon-Rodriguez, L. M.; Lubag, A. J. M.; Malloy, C. R.; Martinez, G. V.; Gillies, R. J.; Sherry, A. D. *Acc. Chem. Res.* **2009**, *42*, 948–957.
- (30) Viswanathan, S.; Kovacs, Z.; Green, K. N.; Ratnakar, S. J.; Sherry, A. D. *Chem. Rev.* **2010**, *110*, 2960–3018.
- (31) Razgulina, A.; Ma, N.; Rao, J. H. *Chem. Soc. Rev.* **2011**, *40*, 4186–4216.
- (32) Verwilt, P.; Park, S.; Yoon, B.; Kim, J. S. *Chem. Soc. Rev.* **2015**, *44*, 1791–1806.
- (33) Sherry, A. D.; Wu, Y. K. *Curr. Opin. Chem. Biol.* **2013**, *17*, 167–174.
- (34) Zhou, X.; Graziani, D.; Pines, A. *Proc. Natl. Acad. Sci. U. S. A.* **2009**, *106*, 16903–16906.
- (35) Berthault, P.; Huber, G.; Desvaux, H. *Prog. Nucl. Magn. Reson. Spectrosc.* **2009**, *55*, 35–60.
- (36) Dybowski, C.; Bansal, N.; Duncan, T. M. *Annu. Rev. Phys. Chem.* **1991**, *42*, 433–464.
- (37) Brotin, T.; Dutasta, J.-P. *Chem. Rev.* **2009**, *109*, 88–130.
- (38) Palaniappan, K. K.; Francis, M. B.; Pines, A.; Wemmer, D. E. *Isr. J. Chem.* **2014**, *54*, 104–112.
- (39) Shapiro, M. G.; Ramirez, R. M.; Sperling, L. J.; Sun, G.; Sun, J.; Pines, A.; Schaffer, D. V.; Bajaj, V. S. *Nat. Chem.* **2014**, *6*, 629–634.
- (40) Bai, Y. B.; Wang, Y. F.; Goulian, M.; Driks, A.; Dmochowski, I. J. *Chem. Sci.* **2014**, *5*, 3197–3203.
- (41) Kunth, M.; Witte, C.; Hennig, A.; Schröder, L. *Chem. Sci.* **2015**, *6*, 6069–6075.
- (42) Kim, B. S.; Ko, Y. H.; Kim, Y.; Lee, H. J.; Selvapalam, N.; Lee, H. C.; Kim, K. *Chem. Commun.* **2008**, 2756–2758.
- (43) Schnurr, M.; Sloniec-Myszk, J.; Döpfert, J.; Schröder, L.; Hennig, A. *Angew. Chem., Int. Ed.* **2015**, *54*, 13444–13447.
- (44) Adiri, T.; Marciano, D.; Cohen, Y. *Chem. Commun.* **2013**, *49*, 7082–7084.
- (45) Berthault, P.; Desvaux, H.; Wendlinger, T.; Gyejacquot, M.; Stopin, A.; Brotin, T.; Dutasta, J.-P.; Boulard, Y. *Chem. - Eur. J.* **2010**, *16*, 12941–12946.
- (46) Riggall, B. A.; Wang, Y.; Dmochowski, I. J. *J. Am. Chem. Soc.* **2015**, *137*, 5542–5548.
- (47) Schröder, L.; Chavez, L.; Meldrum, T.; Smith, M.; Lowery, T. J.; Wemmer, D. E.; Pines, A. *Angew. Chem., Int. Ed.* **2008**, *47*, 4316–4320.
- (48) Schröder, L.; Lowery, T. J.; Hilty, C.; Wemmer, D. E.; Pines, A. *Science* **2006**, *314*, 446–449.

- (49) Spence, M. M.; Ruiz, E. J.; Rubin, S. M.; Lowery, T. J.; Winssinger, N.; Schultz, P. G.; Wemmer, D. E.; Pines, A. *J. Am. Chem. Soc.* **2004**, *126*, 15287–15294.
- (50) Spence, M. M.; Rubin, S. M.; Dimitrov, I. E.; Ruiz, E. J.; Wemmer, D. E.; Pines, A.; Yao, S. Q.; Tian, F.; Schultz, P. G. *Proc. Natl. Acad. Sci. U. S. A.* **2001**, *98*, 10654–10657.
- (51) Seward, G. K.; Wei, Q.; Dmochowski, I. J. *Bioconjugate Chem.* **2008**, *19*, 2129–2135.
- (52) Seward, G. K.; Bai, Y.; Khan, N. S.; Dmochowski, I. J. *Chem. Sci.* **2011**, *2*, 1103–1110.
- (53) Kotera, N.; Dubost, E.; Milanole, G.; Doris, E.; Gravel, E.; Arhel, N.; Brotin, T.; Dutasta, J.-P.; Cochrane, J.; Mari, E.; Boutin, C.; Léonce, E.; Berthault, P.; Rousseau, B. *Chem. Commun.* **2015**, *51*, 11482–11484.
- (54) Khan, N. S.; Riggle, B. A.; Seward, G. K.; Bai, Y.; Dmochowski, I. J. *Bioconjugate Chem.* **2015**, *26*, 101–109.
- (55) Wei, Q.; Seward, G. K.; Hill, P. A.; Patton, B.; Dimitrov, I. E.; Kuzma, N. N.; Dmochowski, I. J. *J. Am. Chem. Soc.* **2006**, *128*, 13274–13283.
- (56) Aaron, J. A.; Chambers, J. M.; Jude, K. M.; Di Costanzo, L.; Dmochowski, I. J.; Christianson, D. W. *J. Am. Chem. Soc.* **2008**, *130*, 6942–6943.
- (57) Chambers, J. M.; Hill, P. A.; Aaron, J. A.; Han, Z.; Christianson, D. W.; Kuzma, N. N.; Dmochowski, I. J. *J. Am. Chem. Soc.* **2009**, *131*, 563–569.
- (58) Roy, V.; Brotin, T.; Dutasta, J.-P.; Charles, M. H.; Delair, T.; Mallet, F.; Huber, G.; Desvaux, H.; Boulard, Y.; Berthault, P. *ChemPhysChem* **2007**, *8*, 2082–2085.
- (59) Kotera, N.; Tassali, N.; Léonce, E.; Boutin, C.; Berthault, P.; Brotin, T.; Dutasta, J.-P.; Delacour, L.; Traoré, T.; Buisson, D. A.; Taran, F.; Coudert, S.; Rousseau, B. *Angew. Chem., Int. Ed.* **2012**, *51*, 4100–4103.
- (60) Tassali, N.; Kotera, N.; Boutin, C.; Léonce, E.; Boulard, Y.; Rousseau, B.; Dubost, E.; Taran, F.; Brotin, T.; Dutasta, J.-P.; Berthault, P. *Anal. Chem.* **2014**, *86*, 1783–1788.
- (61) Zhang, J.; Jiang, W. P.; Luo, Q.; Zhang, X. X.; Guo, Q. N.; Liu, M. L.; Zhou, X. *Talanta* **2014**, *122*, 101–105.
- (62) Witte, C.; Martos, V.; Rose, H. M.; Reinke, S.; Klippel, S.; Schröder, L.; Hackenberger, C. P. R. *Angew. Chem., Int. Ed.* **2015**, *54*, 2806–2810.
- (63) Boutin, C.; Stopin, A.; Lenda, F.; Brotin, T.; Dutasta, J.-P.; Jamin, N.; Sanson, A.; Boulard, Y.; Leteurtre, F.; Huber, G.; Buchmann, A. B.; Tassali, N.; Desvaux, H.; Carrière, M.; Berthault, P. *Bioorg. Med. Chem.* **2011**, *19*, 4135–4143.
- (64) Klippel, S.; Döpfert, J.; Jayapaul, J.; Kunth, M.; Rossella, F.; Schnurr, M.; Witte, C.; Freund, C.; Schröder, L. *Angew. Chem., Int. Ed.* **2014**, *53*, 493–496.
- (65) Rossella, F.; Rose, H. M.; Witte, C.; Jayapaul, J.; Schröder, L. *ChemPlusChem* **2014**, *79*, 1463–1471.
- (66) Rose, H. M.; Witte, C.; Rossella, F.; Klippel, S.; Freund, C.; Schröder, L. *Proc. Natl. Acad. Sci. U. S. A.* **2014**, *111*, 11697–11702.
- (67) Dubost, E.; Dognon, J.-P.; Rousseau, B.; Milanole, G.; Dugave, C.; Boulard, Y.; Lonce, E.; Boutin, C.; Berthault, P. *Angew. Chem., Int. Ed.* **2014**, *53*, 9837–9840.
- (68) Leonard, N. J.; Ning, R. Y. *J. Org. Chem.* **1966**, *31*, 3928–3935.
- (69) Iciek, M.; Chwatko, G.; Lorenc-Koci, E.; Bald, E.; Wlodek, L. *Acta Biochim. Polym.* **2004**, *51*, 815–824.
- (70) Yang, X. F.; Guo, Y. X.; Strongin, R. M. *Angew. Chem., Int. Ed.* **2011**, *50*, 10690–10693.
- (71) Guo, Z. Q.; Nam, S. W.; Park, S.; Yoon, J. Y. *Chem. Sci.* **2012**, *3*, 2760–2765.
- (72) Park, S.; Imlay, J. A. *J. Bacteriol.* **2003**, *185*, 1942–1950.
- (73) Dethlefseni, L. A.; Biaglow, J. E.; Peck, V. M.; Ridinger, D. N. *J. Cell. Physiol.* **1987**, *132*, 149–154.